Since January 2020 Elsevier has created a COVID-19 resource centre with free information in English and Mandarin on the novel coronavirus COVID-19. The COVID-19 resource centre is hosted on Elsevier Connect, the company's public news and information website.

Drug Metabolism and Pharmacokinetics 44 (2022) 100450

Contents lists available at ScienceDirect

Drug Metabolism and Pharmacokinetics

journal homepage: http://www.journals.elsevier.com/drug-metabolism-and-pharmacokinetics

Review

Recent advances in lipid nanoparticles for delivery of nucleic acid, mRNA, and gene editing-based therapeutics

Hidefumi Mukai [a, b, *], Koki Ogawa [a, 1], Naoya Kato [a, 1], Shigeru Kawakami [a, **]

[a] Department of Pharmaceutical Informatics, Graduate School of Biomedical Sciences, Nagasaki University, 1-7-1 Sakamoto, Nagasaki-shi, Nagasaki, 852-8588, Japan
[b] Laboratory for Molecular Delivery and Imaging Technology, RIKEN Center for Biosystems Dynamics Research, 6-7-3 Minatojima-minamimachi, Chuo-ku, Kobe, Hyogo, 650-0047, Japan

ARTICLE INFO

Article history:
Received 15 October 2021
Received in revised form
30 January 2022
Accepted 1 February 2022
Available online 5 February 2022

Keywords:
Lipid nanoparticle
Nucleic acid
mRNA
Gene editing
Base editing
Ionizable lipid
Targeting
DNA barcode
Recombination
Positron emission tomography

ABSTRACT

Lipid nanoparticles (LNPs) are becoming popular as a means of delivering therapeutics, including those based on nucleic acids and mRNA. The mRNA-based coronavirus disease 2019 vaccines are perfect examples to highlight the role played by drug delivery systems in advancing human health. The fundamentals of LNPs for the delivery of nucleic acid- and mRNA-based therapeutics, are well established. Thus, future research on LNPs will focus on addressing the following: expanding the scope of drug delivery to different constituents of the human body, expanding the number of diseases that can be targeted, and studying the change in the pharmacokinetics of LNPs under physiological and pathological conditions. This review article provides an overview of recent advances aimed at expanding the application of LNPs, focusing on the pharmacokinetics and advantages of LNPs. In addition, analytical techniques, library construction and screening, rational design, active targeting, and applicability to gene editing therapy have also been discussed.

1. Introduction

Lipid nanoparticles (LNPs) are becoming popular as delivery agents for nucleic acid and mRNA-based therapeutics [1–4]. This follows a series of clinical successes beginning with patisiran (Onpattro®), the first approved RNA interference drug [3,5]. Particularly, the mRNA coronavirus disease 2019 (COVID-19) vaccines marketed by Moderna and Pfizer, are a great example to show how research and development of drug delivery systems (DDSs) over the years has contributed to the health and welfare of humanity [6,7].

LNPs refer to all nanoparticles composed of lipids, including a variety of classes such as liposomes. Nowadays, the term is often used to refer to stable nucleic acid-lipid nanoparticles, particularly in the field of nucleic acid and mRNA DDSs; therefore, this article follows this narrow usage. The strategy for developing LNPs for delivering nucleic acid and mRNA-based therapeutics has been fairly established, and several review articles focusing on the concepts, basic components, and fundamental technologies have already been published [1–4,8–10]. Thus, they are only briefly described here.

Ionizable lipids play a critical role in LNPs [11–13]. Dlin-MC3-DMA [14], used in patisiran, SM-102 [15] and *SS*-cleavable pH-activated lipid-like material (ssPalm) [16,17], which are biodegradable lipids, and lipidoid C12-200 [18–20] are a few examples for this. In addition to the encapsulation of nucleic acids and

* Corresponding author. Department of Pharmaceutical Informatics, Graduate School of Biomedical Sciences, Nagasaki University, 1-7-1 Sakamoto, Nagasaki-shi, Nagasaki, 852-8588, Japan.
** Corresponding author.
E-mail addresses: hmukai@nagasaki-u.ac.jp (H. Mukai), skawakam@nagasaki-u.ac.jp (S. Kawakami).
[1] Contributed equally to this work.

https://doi.org/10.1016/j.dmpk.2022.100450
1347-4367/

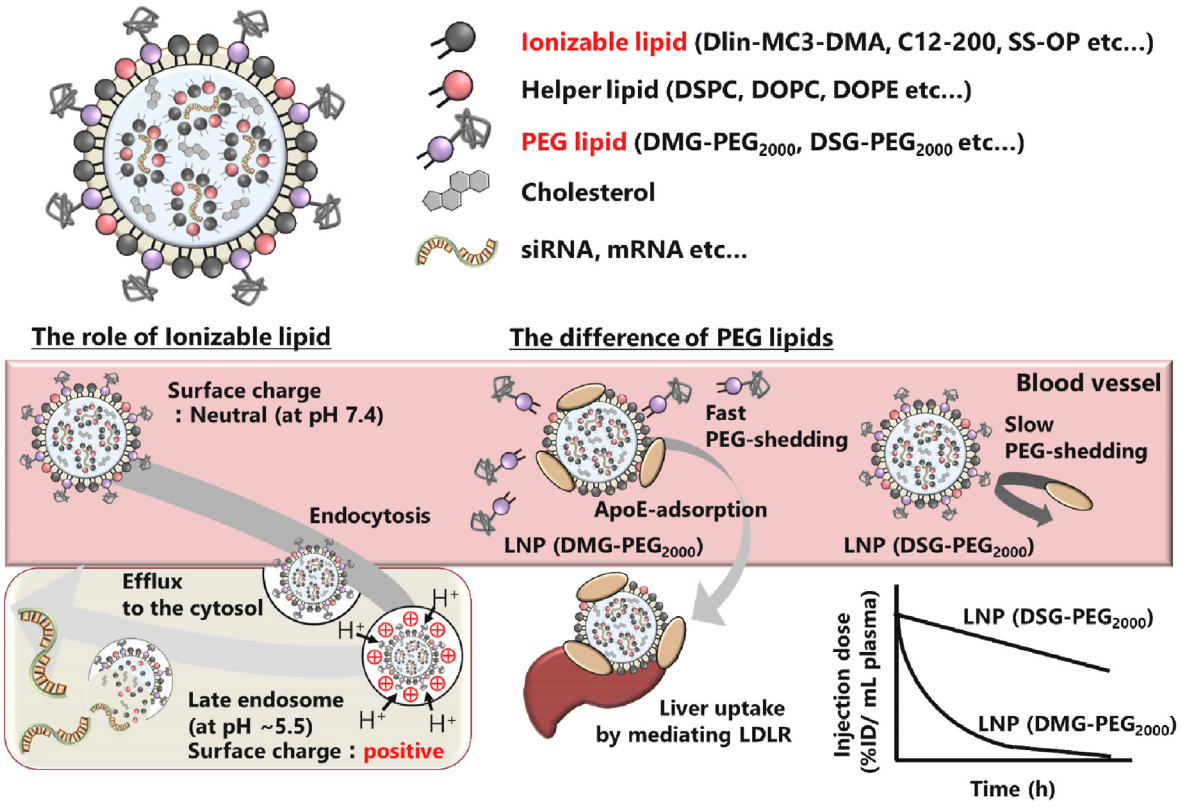

Fig. 1. The concepts, basic components, and fundamental technologies of lipid nanoparticles for delivery of nucleic acid and mRNA-based therapeutics. Nucleic acids and mRNAs are in the lipid cores of LNPs; the outer lipid membranes of LNPs are not perfectly aligned bilayers like liposomes, but are close to micelles in structure. Ionizable lipids contribute to efficient endosomal escape and release of nucleic acids and mRNAs from LNPs after uptake by cells, in addition to the encapsulation of nucleic acids and mRNAs into LNPs. The LNPs modified with 1,2-dimyristoyl-rac-*glycero*-3-methoxypolyethylene glycol-2000 (DMG-PEG) can detach PEG at a moderate rate in the blood circulation, resulting in efficient intracellular delivery of nucleic acids and mRNAs. The uptake of LNPs in the hepatocytes, after the intravenous administration, is caused via the low-density lipoprotein receptor (LDLR) because of the interaction between LNPs and apolipoprotein E (apoE) in the blood.

mRNAs into LNPs, ionizable lipids contribute to efficient endosomal escape and release of nucleic acids and mRNAs from LNPs after uptake by cells (Fig. 1) [12]. One of the major challenges in designing DDS was that polyethylene glycol (PEG) modification improved the blood stability of nanoparticle formulations after systemic administration, but also inhibited their uptake into target cells [21–23]. A simple strategy to overcome this problem was the development of 1,2-dimyristoyl-rac-*glycero*-3-methoxypolyethyl ene glycol-2000 (DMG-PEG), in which the alkyl tail of the PEG-lipid is shortened to C14 from that of the conventional type (Fig. 1) [24]. The LNPs modified with DMG-PEG can detach PEG at a moderate rate in the blood circulation, resulting in efficient intracellular delivery of nucleic acids and mRNAs [24–26]. Furthermore, by applying microfluidic technologies such as the T-mixer, a technology to efficiently mix lipids with nucleic acids or mRNAs was developed, which has enabled us to produce LNPs with a high degree of reproducibility [27–29]. LNP technology has become a powerful tool in drug development. Using advanced analytical techniques such as cryogenic electron microscopy and small angle X-ray scattering, the structure of LNPs has been elucidated. LNPs are characterized by the absence of a distinct inner aqueous phase, unlike traditional unilamellar and multilamellar liposomes, which possess a distinct inner aqueous phase [30]. Nucleic acids and mRNAs are in the lipid cores of LNPs; the outer lipid membranes of LNPs are not necessarily perfectly aligned bilayers like liposomes, but are close to micelles in structure (Fig. 1) [1,31,32].

This review article will provide an overview of the pharmacokinetics of LNPs, and the research and development aimed at expanding the applications of LNPs, with particular emphasis on recent advances.

2. General pharmacokinetics of LNPs and their analytical techniques

Optical imaging has become the method of choice for pharmacokinetic analysis of nanoparticular and other formulations, due to its high accessibility and throughput. This is despite the fact that it is only semi-quantitative in nature, as it is a two-dimensional imaging technique [33]. While autofluorescence is often a problem with fluorescence imaging, luminescence imaging can, in principle, be expected to have an extremely high signal-to-noise ratio. Recent improvements in charge-coupled device cameras have made them more sensitive. Particularly in the development of gene and mRNA therapeutics, luminescence imaging has been widely used to evaluate the tissue distribution of exogenous protein expression and its change over time in the same individual, using luciferase as a reporter [34,35]. The protein expression characteristics of standard mRNA/LNPs have been reported after their administration through several routes [34,35]. Pardi et al. reported the mRNA translation patterns in mice of the LNPs (~80 nm in size) that consisted of ionizable cationic lipid, phosphatidylcholine, cholesterol, and PEG-lipid (50/10/38.5/1.5 M ratio) and luciferase mRNA (RNA/total lipid ratio of ~0.05 wt/wt) [34]. The ionizable cationic lipid and PEG-lipid were not clearly mentioned in their work, but DLin-MC3-DMA or its analogs, and PEG-DMG were probably used, respectively. It was reported that mRNA translation (luciferase

expression) after intravenous administration of mRNA/LNPs was mainly in the liver, and that it frequently occurred even after local administration through intraperitoneal, intramuscular, subcutaneous, intradermal, and intratracheal routes, because a portion of the mRNA/LNPs entered the systemic circulation. Interestingly, the duration of mRNA translation varied among organs and tissues. It rapidly declined in the liver, while intramuscular and intradermal mRNA translation tended to be relatively persistent, and was observed for up to a week. Intranasal administration was also evaluated using a similar approach in another paper, which reported no mRNA translation [35], although it may vary with administration technique and condition. Recently, luciferin analogs generating near-infrared luminescence were developed [36,37]. The increasing sensitivity of luminescence imaging may, for example, make it possible to evaluate the efficiency of exogenous protein expression in deeper organs and tissues with lower levels of protein expression.

The high and specific uptake of LNPs in the liver, especially in the hepatocytes, after this intravenous administration, was shown to be caused via the low-density lipoprotein receptor (LDLR) because of the strong interaction between LNPs and apolipoprotein E (apoE) in the blood (Fig. 1) [38]. The interaction of nanoparticle formulations with cells and proteins in blood has long been discussed [39–41]. Recently, proteins bound to LNPs, called protein corona or biomolecular corona because of their shape, have been the subject of much research attention as factors that contribute greatly to LNP pharmacokinetics [42–45]. The latest findings concerning protein coronas of LNPs, including the analytical technical aspects, were recently reviewed [46]. Although there are still many unknowns owing to the immaturity of the technology, a list of constituents of protein coronas has been developed, that includes serum albumin, complement factors, immunoglobulins, and apolipoproteins. Proteins present in smaller quantities may be important; improving the methods of separation of LNP-protein corona complexes and the sophistication of proteomics technology are key to a more detailed analysis of the protein coronas. The physiological and pathological conditions of patients and animal models, and the route of administration, and their impact on pharmacokinetics are also important factors to consider.

For a detailed analysis of the intratissue distribution of LNPs, a method that makes use of the Cre/loxP recombinase system is beginning to be used [47–49]. This method uses transgenic mice that have reporter genes (especially fluorescent proteins) downstream of the loxP-flanked stop cassette, which blocks reporter gene expression in the absence of cyclization recombinase (Cre) in the cells, but in the presence of Cre, the stop cassette is removed, and the gene is expressed (Fig. 2) [50]. For example, the typical Ai14 mouse has Lox-Stop-Lox-tdTomato (LSL-tdTomato) inserted into the Rosa26 region, which is a known safe harbor locus for gene insertion into the mouse genome [50]. These mice can be crossed with other transgenic mice that express Cre in a cell type-selective manner and have been widely used to generate model mice in which specific cell types are labeled with fluorescence [51,52]. Treatment of these mice with LNPs encapsulating mRNA-encoding Cre results in stable expression of fluorescent protein in the delivered cells selectively. To be precise, only cells that have undergone all the following steps are fluorescently labeled: (1) mRNA is transferred to the cytoplasm, (2) Cre protein is produced by translation, (3) Cre is transferred to the nucleus, and (4) the stop cassette is removed by recombination. It is useful for identifying delivered cells and quantifying the delivery efficiency of each cell type and is particularly convenient, in that, traces of Cre mRNA translation and its functional expression are stably labeled with fluorescence. This allows evaluation without optimization of the timing of protein production. However, it should be noted that the disadvantage of this method is that it does not allow for the quantification of the expression levels of foreign proteins and their changes over time. An example of the use of this method was in evaluating the mRNA delivery efficiency to each cell type in tissues [47]. This was done by separating the liver, lung, and spleen cells into hepatocytes, liver sinusoidal endothelial cells, and Kupffer cells; epithelial cells and endothelial cells; B cells, T cells, and macrophages, respectively, using flow cytometry. In addition, in the development of LNPs targeting the brain, a clear demonstration of mRNA delivery beyond the blood-brain barrier (BBB) to the cells in cerebral cortex, hippocampus, and cerebellum would also be an example of effective application [48]. Although the introduction of transgenic mice is a hurdle, it is expected to become one of the popular methods of biodistribution analysis in the future.

Positron emission tomography (PET) is an imaging technique that can be used seamlessly from rodents to humans. Its application to pharmacokinetic research and drug development has been explored, owing to its high quantitative and temporal resolution [33,53–56]. The ability to directly evaluate drug concentrations in

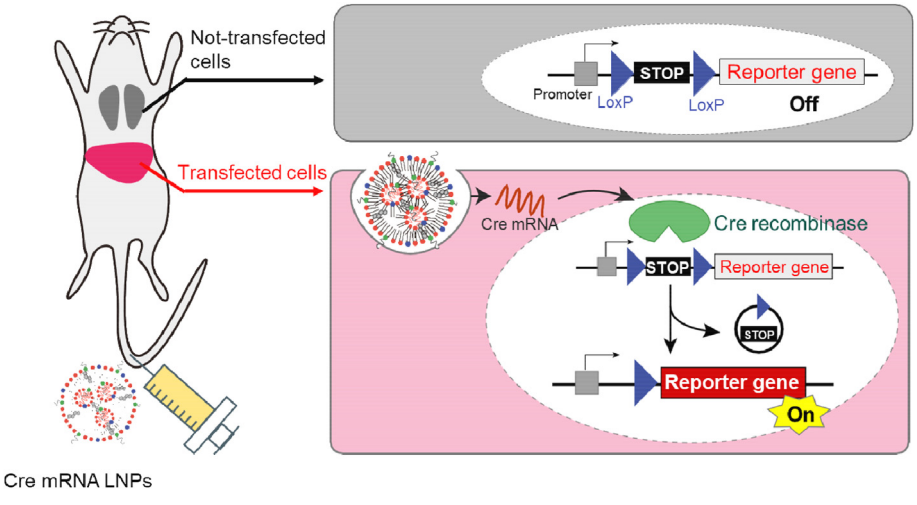

Fig. 2. Analysis of the intratissue distribution of LNPs using the Cre/loxP recombinase system. The transgenic mice that have reporter genes downstream of the loxP-flanked stop cassette, blocks reporter gene expression in the absence of cyclization recombinase (Cre) in the cells, but in the presence of Cre, the stop cassette is removed, and the gene is expressed. Treatment of these mice with LNPs encapsulating mRNA-encoding Cre results in stable expression of fluorescent protein in the delivered cells selectively.

human tissues, which was previously impossible, is a breakthrough [53–56], and is expected to lead to efficient drug development that strongly links pharmacokinetics to drug efficacy. Although small molecule and antibody drugs have been the main targets so far, application of PET has recently been expanded to include nucleic acid drugs and their DDS formulations [53–66]. Positron emitter labeling methods with ^{18}F and ^{64}Cu have been established for nucleic acid therapeutics such as antisense drugs [62–66], and the pharmacokinetic evaluation of DDS formulations of nucleic acid therapeutics using PET has been reported [65,66]. For example, Mukai et al. evaluated the pharmacokinetics of a liposomal formulation encapsulating phosphorothioate antisense oligodeoxynucleotides (ODNs) in a xenograft mouse model of human pancreatic cancer cell line [65]. In this study, the authors combined dynamic PET imaging, which can obtain highly sensitive and time-resolved pharmacokinetic data over time in the same individual, with LC/MS/MS, which can separately evaluate the intact drug and its metabolites. The results demonstrated the in vivo nucleic acid protective effect of the liposome formulation and the delivery of intact ODNs to the tumors. In addition, based on the intact/accumulated ODN ratio (calculated by dividing the tissue drug concentrations by LC/MS/MS analysis by those by PET analysis), it was found that the liposomal formulation effectively protected ODNs in blood, tumors, and kidneys, while the protective effect was very low in the liver, resulting in the rapid degradation of ODNs.

Furthermore, PET-based pharmacokinetic evaluation of mRNA/cholesterol-kanamycin lipidic derivatives complex were reported [66]. The conventional positron emitter-labeling approaches are not applicable to mRNAs synthesized by in vitro transcription, because they essentially lack reactive functional groups suitable for chemical modification of chelators. In their paper, Lindsay et al. prepared positron emitter-labeled mRNA by a slightly complex but unique method, in which mRNA was allowed to form complementary strands with biotin-modified oligonucleotides, and then bound with ^{64}Cu-labeled NeutrAvidin. Biodistribution data based on PET-computed tomography were obtained over 28 h after administration of ^{64}Cu-labeled mRNA/cholesterol-kanamycin lipidic derivatives complex to quadriceps of Cynomolgus macaques. With the passage of time, an increase in the accumulation in draining lymph nodes was observed, which probably reflects the migration process following the uptake of the nanoparticle formulation by the antigen-presenting cells. The nanoparticular formulations were labeled with near-infrared fluorescent dye in addition to the positron emitter; the tissues with efficient uptake were excised under the fluorescence imaging guide; and their distribution was evaluated at the cell-type level by flow cytometry. Furthermore, the yellow fever *prME* mRNA was labeled in a translatable form, which allowed immunological evaluation. Such a combined experimental design will be useful for analyzing the correlation between pharmacokinetics and drug efficacy in the same individual in preclinical studies, especially using non-human primates in vaccine development, where individual differences are likely to occur.

3. Advantages of LNPs: library construction and screening

Current pharmacokinetic knowledge is still insufficient to develop the delivery system of nucleic acid therapeutics, which must overcome the multi-step obstacles described above, to target organs/tissues and cells in a fully rational manner. Thus, screening approaches can be particularly powerful, as in the discovery of lead compounds for drugs based on small molecules and antibodies. To identify efficient delivery systems, the construction of their libraries with sufficient diversity and appropriate screening indices that are easily quantifiable, are essential. With LNP, the key components were narrowed down, and the preparations were simplified to mixing, which makes it easier to construct libraries with sizes greater than dozens. In addition, high-throughput screening is possible with deep sequencing of nucleic acids using next-generation sequencers, as described below [67–72]. Through such screening, the data on lipid structure/composition-protein production/gene silencing activity relationships is being accumulated, which is expected to lead to the rational design of LNPs in future.

Among the components of LNPs, particular emphasis has been placed on the screening of ionizable lipids [11–20]. One of the earliest examples was the ionizable amino lipid screening for siRNA delivery to the liver, which led to the first RNAi therapeutic, patisiran (Onpattro®) [14]. Fifty-six amino lipids with the common dilinoleyl tails and varied amine head groups and linkers were synthesized, and a library of LNPs containing each amino lipid with distearoylphosphatidylcholine (DSPC), cholesterol, and (*R*)-2,3-bis(octadecyloxy)propyl-1-(methoxy poly (ethylene glycol)2000) propylcarbamate (PEG-DMG) was constructed. The screening was based on the median effective doses (ED_{50}) of factor VII gene knockdown (measuring factor VII protein in serum) after intravenous administration of the LNP encapsulating factor VII siRNA; the most efficient ionizable lipid was found to be (6*Z*,9*Z*,28*Z*,31*Z*)-heptatriaconta-6,9,28,31-tetraen-19-yl 4-(dimethylamino)butanoate (DLin-MC3-DMA). This lipid is still one of the gold standards, and is used for comparison in the performance evaluation of many subsequent LNPs. In this study, the apparent acid dissociation constants (pK_a) of amino lipids that exist in LNPs were determined using the change in fluorescence of 2-(*p*-toluidino)-6-naphthalene sulfonic acid (TNS) with pH titration, and their correlation with the gene knockdown efficiencies was investigated. The resulting correlation was sharp bell-shaped, and the finding was that the optimal range of pK_a is very narrow, between 6.2 and 6.5. In contrast, even in that range, the ED_{50} values can vary by up to a factor of 15, indicating that a completely rational design of LNPs is difficult to achieve.

The screening process for SM-102, the ionizable lipid used in the COVID-19 vaccine developed by Moderna, has also been published [15]. For the LNP library for intramuscularly administered mRNA vaccines, lipids containing esters in their tails and tertiary amines as ionization sites were used to enable rapid metabolism in vivo. This was done to increase the focus on reducing adverse effects. Thirty different LNPs co-encapsulating luciferase mRNA and H10N8 influenza hemagglutinin antigen mRNA, were administered intramuscularly to mice and screened by simultaneously evaluating protein production and immune induction. Five candidates were selected, and SM-102 was finally chosen as the lipid to be used in clinical LNPs based on the subsequent studies of tolerability and other factors. Interestingly, it is reported that the optimal lipid pK_a for immune induction was in the range of 6.6–6.8, unlike in the case of siRNA delivery to the liver, and that there was no strong correlation between protein production levels and immune induction. This could be because lipids have the effect of an adjuvant. In addition, the LNPs that result in high protein production tend to be somewhat similar, but not identical, between the intravenous and intramuscular administration.

Currently, LNPs targeting various organs/tissues, and each group of cells constituting the liver other than hepatocytes are being developed, where there is no easy-to-use index for screening such as the factor VII gene knockdown mentioned above. Therefore, versatile, quantitative, reproducible, and high-throughput methods for evaluating their biodistributions are essential. For this reason, DNA barcode technologies are beginning to be used [67–72].

DNA barcoding was originally a phylogenetic method in biology that used short genetic markers to identify species from DNA

sequences [73,74]. It has now become powerful with the advent of next-generation sequencing technology. This approach can also be applied to materials and has been proposed for use in high-throughput screening of DDS formulations based on their biodistribution [67–72]. LNPs with different compositions encapsulating nucleic acids with individual DNA or RNA sequences assigned to each as barcodes are prepared and made into libraries (Fig. 3). By administering the mixture of these barcoded LNPs to experimental animals and performing deep sequencing for DNA or RNA barcode in each tissue, the tissue distribution characteristics of LNPs with each lipid composition can be quantified at once. This is highly effective for the high-throughput screening of LNPs suitable for targeting each organ/tissue. This approach leads to a reduction in the number of animals used, direct comparisons of LNP biodistributions on the same individuals, and a reduction in experimental effort. These factors make DNA barcoding very suitable for the development of DDS technologies such as LNPs for drugs based on nucleic acids and mRNA.

A proof-of-concept for the screening of LNPs with DNA barcodes was obtained in the simultaneous evaluation of 30 different LNPs for their distribution in eight tissues [67]. The DNA barcodes used were 61 nucleotides long, including a barcode sequence of 10 nucleotides near the middle, and Illumina adapter sequences of approximately 20 nucleotides at each of the 5′ and 3′ ends. The three nucleotides at both ends of the DNA barcodes were modified with phosphorothioate so that they were not degraded by exonuclease. Although the detection sensitivity depends on the devices and sequencing conditions, the conditions in this study, which used Illumina MiSeq, were highly sensitive. In the evaluation of LNPs containing C12-200 having a complex structure with five alkyl chains as an ionizable lipid-like molecule, there was a linearity between dose and liver DNA barcode counts in the dose range of 0.0001–0.5 mg/kg. Depending on the accumulation of LNPs in the target tissues, this linearity with low dose and wide range indicated that the tissue distribution characteristics of dozens or hundreds of LNPs can be evaluated in the same mouse at a time. As a demonstration of this method, 30 types of LNPs containing C12-200 with different molecular weights and lengths of alkyl chain tails of PEG-lipids and their molar ratios were evaluated for their distributions in the heart, brain, uterus, muscle, kidney, pancreas, liver, and lung. Data with very low variance were obtained even with 3–4 replicates of animals, indicating high reproducibility of this method. Since the ultimate function of LNPs is target gene knockdown or exogenous gene expression, and these evaluations are necessary, it is reasonable that this method is used to exclude LNPs that do not function effectively. In fact, there was an approximate correlation between the number of DNA barcodes counted in the liver after administration of each LNP, and the decrease in its protein concentration in the blood when factor VII siRNA was delivered with the corresponding LNPs. This strongly suggests that this method can function effectively as a first-pass screening of LNPs.

An example of using this method to evaluate the tissue distribution of LNPs on a larger scale is a comparison in the library that consisted of 96 LNPs based on the ionized lipid-like molecule C12-200, with different helper lipid types, molar ratios of cholesterol, molecular weights of PEG-lipids, and mixing ratios of lipids and

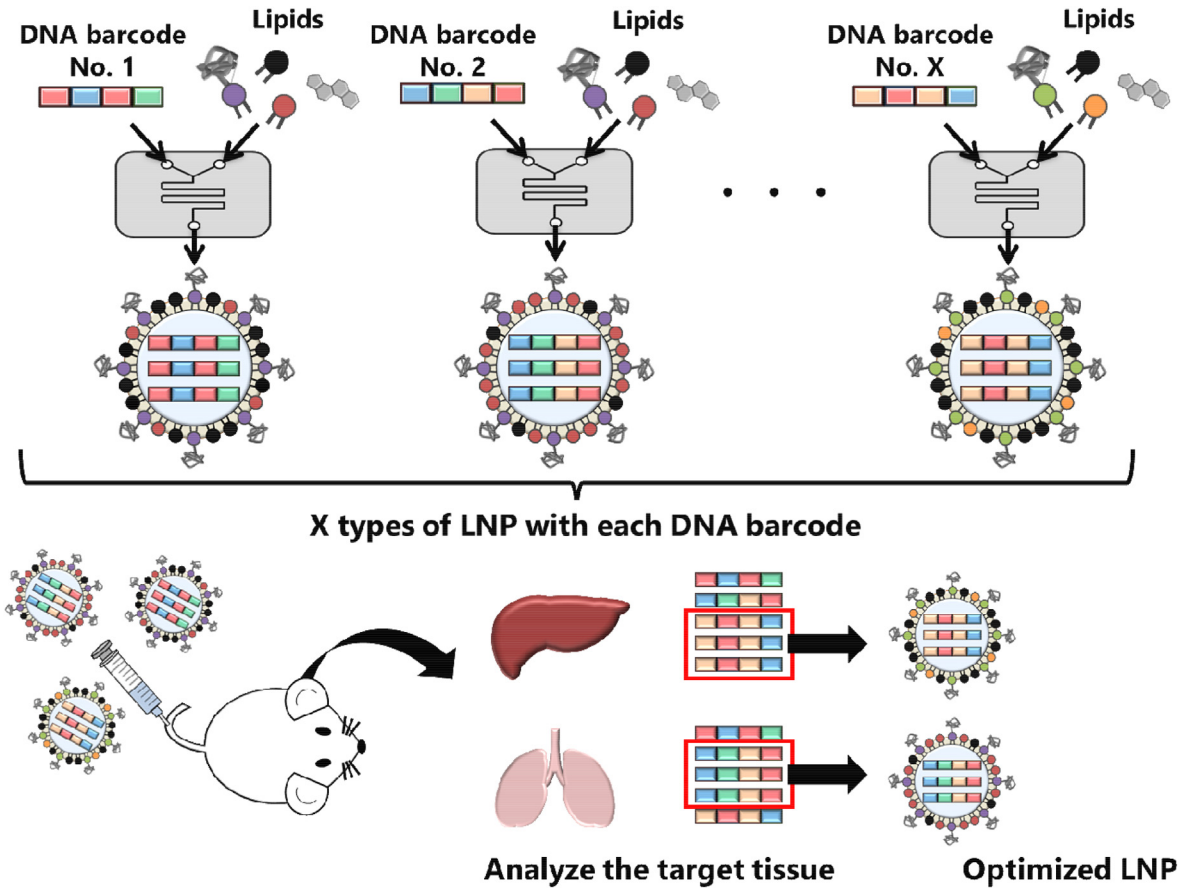

Fig. 3. High-throughput screening of LNPs suitable for targeting each organ/tissue using DNA barcoding. LNPs with different compositions encapsulating nucleic acids with individual DNA or RNA sequences assigned to each as barcodes are prepared and made into libraries. By administering the mixture of these barcoded LNPs to experimental animals and performing deep sequencing for DNA or RNA barcode in each tissue, the tissue distribution characteristics of LNPs with each lipid composition can be quantified at once.

DNA [69]. This systematic evaluation suggested that helper lipids, which have not received much attention so far, may affect the tissue accumulation characteristics of LNPs. Specifically, LNPs that contain DOPE as a helper lipid tended to accumulate in the liver, while LNPs that contain DSPC accumulated preferentially in the spleen. Using the technique of quartz crystal microbalance with dissipation monitoring, the LNPs that contain DSPC as a helper lipid were shown to have a significantly weaker interaction with ApoE. This may be an example of how high-throughput screening reveals new factors that need to be optimized for the rational design of LNPs. In addition, for the development of LNPs for mRNA drugs, the construction and use of LNP libraries using barcoded mRNA, instead of DNA barcodes, are desirable because they allow for more accurate evaluation of mRNA/LNPs biodistribution. The library construction of in vitro transcripted mRNAs having 10 nucleotides of barcode sequences and unique molecular identifiers (UMIs), which reduce errors caused by amplification and quantitative biases behind the sequence of gene of interest have been reported [70]. This study showed that the tissue distribution characteristics of barcoded mRNA (typically hundreds to thousands of nucleotides) and DNA barcodes (61 nucleotides) were different, despite LNPs with identical formulation parameters, strongly suggesting the importance of using barcoded mRNA.

The DNA/RNA barcode-based screening not only evaluates biodistribution at the tissue level, but also at the cell-type level in more detail when combined with flow cytometry. In addition, by combining this with the Cre/loxP recombinase system described above, in which cells expressing foreign Cre proteins above a certain threshold were fluorescently labeled, a high-throughput evaluation of not only mRNA delivery, but also of foreign protein expression was reported [71]. Specifically, a library of 75 LNPs, encapsulating DNA barcodes and Cre mRNA together, was constructed and administered to Ai14 mice carrying the LSL-tdTomato cassette. By flow cytometry selection of tdTomato-positive cells, and further immunostaining with various cell markers, a total of 28 cell types from 7 tissues were isolated and amounts of DNA barcodes were quantified for each, using next generation sequencing. This method allows us to focus on the LNPs that ultimately result in Cre protein expression. Thus, its advantage is that LNPs that are taken up by the cell but have low protein expression efficiency are excluded in principle. Interestingly, a distinctive study was conducted using a library of LNPs based on nine cholesterol derivatives, and cluster analysis suggested that oxidative modification of the hydrocarbon tail adjacent to sterol ring D (for example, 20α-hydroxycholesterol) may be effective for mRNA delivery to the Kupffer and hepatic endothelial cells. Moreover, it is worth mentioning that the development of a more sensitive method for biodistribution evaluation of LNPs, named quantitative analysis of nucleic acid therapeutics, was reported by applying digital droplet PCR for absolute quantification [72]. Digital droplet PCR is usually used to quantify rare genomic events [75].

4. Rational design and active targeting

Till date, there are only a few successful examples of rational LNP design; the following are some examples of tuning tissue selectivity by charge control [47] and conferring cell selectivity by small molecule ligand modification [48,49,76] or antibody [77–81].

The charge of nanoparticles has been well known to change their tissue selectivity after intravenous administration, as exemplified in liposome formulations [82–84]. Applying this pharmacokinetic knowledge, several tissue-targeted LNPs have been developed by adding cationic or anionic lipids to the general composition of LNPs to tune their charge [47]. Specifically, based on the LNPs composed of dendrimer-type ionizable lipid, DOPE, cholesterol, and DMG-PEG (15/15/30/3 molar ratio), (which was optimized for efficient mRNA delivery to the liver), the mixing ratio of an additional lipid, 1,2-dioleoyl-3-trimethylammonium-propane (DOTAP), (which is cationic under physiological conditions because of its quaternary amine), gradually increased. Although the original LNPs predominantly expressed the luciferase reporter in the liver, its expression in the spleen became higher by adding 10–15% DOTAP; more than 90% of the expression was in the lung by adding 30–40% or more DOTAP. On the other hand, the addition of 10–30% of 1,2-dioleoyl-*sn*-glycero-3-phosphate (18 PA), which is a negatively charged lipid, resulted in an almost complete change to the spleen-targeting LNPs. The particle sizes of lung-targeting LNPs (50% DOTAP) and spleen-targeting LNPs (30% 18 PA) were 113.1 nm (PdI, 0.22) and 142.1 nm (PdI, 0.13), respectively. There were minimal changes from those of their original LNPs, 93.2 nm (PdI, 0.14). The zeta-potentials of the original, lung-targeting, spleen-targeting LNPs were between −0 and −3.6 mV and almost unchanged. In addition, with any of the LNPs, mRNA doses of 0.01–0.3 mg/kg were reported to produce therapeutic blood levels of human erythropoietin, mouse interleukin-10, and other therapeutic proteins. Furthermore, in this study, a more detailed evaluation of the mRNA-transfected cell types and their percentages was performed by flow cytometry in the abovementioned transgenic mice, whose cells have the property of being labeled with tdTomato upon recombination by exogenous Cre protein expression. The results showed that lung-targeted LNPs transfected mRNA to ~40%, ~65%, and ~20% of lung epithelial cells, endothelial cells, and immune cells, respectively; the spleen-targeted LNPs transfected mRNA to ~12%, ~10%, and ~20% of B cells, T cells, and macrophages, respectively. Within these cells, lung epithelial cells are targets for cystic fibrosis therapy; B cells for Non-Hodgkin's B-cell lymphoma therapy. The authors showed that this method can be applied to LNPs with other ionizable lipids, including DLin-MC3-DMA. They named it selective organ targeting (SORT) as a general strategy that allows LNPs developed to target the liver, to be easily converted to those targeting the lung or spleen. It has been speculated that the differences in the formation of protein coronas may cause this tissue selectivity; however, it may not be easy to expand the number of target organs beyond the lungs and spleen, which are considered relatively easy to target in conventional DDS development.

Taking advantage of the presence of specific sugar receptors on the surface of cells, depending on the cell types, sugar modifications have been studied as active targeting strategies for nanoparticle formulations such as liposomes [84–89]. In particular, mannose receptors (CD206) have been attracting attention because they are expressed on immunocompetent cells such as macrophages and dendritic cells, as well as on vascular endothelial cells [90]. Applying this strategy, an attempt to modify the cell selectivity in the liver by mannose modification was also reported in LNPs [49]. The pharmacokinetics of general LNPs is determined by the formation of protein corona especially after systemic administration, as described above. To make active targeting dominant, it is necessary to inhibit the formation of protein corona. It has been reported that increasing the amount of PEG-lipids reduced the interaction with ApoE and the LDLR-mediated delivery to hepatocytes. Therefore, in the LNPs based on ionizable lipids, DOPE, cholesterol, and PEG-lipid, the amount of PEG-lipid was increased to 3%, which is higher than general LNPs, and 2.5% of it was replaced with mannose-modified PEG-lipid. In the evaluation of firefly luciferase mRNA as a reporter, the mannose modification of LNPs did not change the liver-specific protein expression. The cellular pattern of protein expression in the liver, however, changed significantly in an evaluation using LSL-tdTomato mice. In the original LNPs, the percentage of tdTomato-positive cells was ~70% for hepatocytes, ~10% for liver sinusoidal endothelial cells (LSECs),

and ~5% for Kupffer cells; in the mannose-modified LNPs, the percentage was ~15% for hepatocytes, ~70% for LSECs, and ~15% for Kupffer cells. Using these mannose-modified LNPs, a single intravenous dose of 0.5 mg/kg siRNA was reported to reduce the serum concentration of factor VIII, which is mainly produced by LSECs, by nearly 10%. Notably, its significant reduction was not observed in the original LNPs. In this report, the mannose modification changed their particle sizes from ~40 nm to ~100 nm, and this difference may also contribute to LSEC targeting. By using galactose-modified LNPs as a control, it was demonstrated that the ApoE protein corona-mediated uptake of LNPs can be switched to active targeting via receptor-mediated endocytosis. In addition, the effect of active targeting by mannose modification to LNPs has been investigated in intramuscularly and intradermally administered mRNA vaccines using mannose-cholesterol amine conjugate, which enhanced the induction of liquid and cellular immunities [76].

Another example is the brain-targeting LNPs modified with neurotransmitters, which are known to penetrate the BBB [48]. Specifically, the lipidoid NT1-O14B having tryptamine, a neurotransmitter, in its head and two alkyl chains in its tail connected by disulfide and ester bonds was developed. For preparation of antisense oligonucleotides-encapsulating LNPs, NT1-O14B was mixed with 306-O12B-3, a bioreducible and biodegradable lipid with disulfide and ester bonds. 306-O12B-3 has been demonstrated to be useful in the LNP-based delivery of antisense oligonucleotides, in a 3:7 wt ratio, in addition to 4 wt % of DSPE-PEG2000. The LNPs generated to demonstrate the knockdown of tau (whose abnormal phosphorylation causes neurofibrillary changes and is believed to be one of the factors in Alzheimer's disease), had a particle size of ~175 nm (PdI, a little less than 0.2) and a zeta-potential of approximately −15 mV. Intravenous administration of these LNPs at a dose of 1 mg/kg antisense oligonucleotide, five times with 3-day intervals reduced Tau mRNA in the brain by about half. Furthermore, the delivery to the cerebral cortex, cerebellum, and hippocampus was demonstrated by the experiment in which Ai14 mice were treated with the LNPs encapsulating negatively supercharged (−27)GFP-Cre protein, and the distribution of tdTomato-labeled cells in the brain was investigated. Although the detailed mechanism has not been reported, these results demonstrated that LNPs were able to cross the BBB while maintaining their structures for delivering cargos to the cytoplasm of neural cells. It has been shown that the optimized ratio of the two lipidoids, NT1-O14B and 306-O12B-3, is essential for efficient delivery to the neuronal cells. Such precise design may be important to achieve a good balance between transcytosis in the BBB and membrane fusion in the neural cells. Although these efforts are still in their infancy, the development of LNPs that can cross the BBB and deliver nucleic acids and mRNA therapeutics to neurons, astrocytes, microglia, and other neural cells that are therapeutic targets for brain diseases, will be one of the major challenges in the field of DDS.

Modification with antibodies is a versatile way to endow active targeting abilities to nanoparticle formulations [91–93], and it is beginning to be reported for LNPs. A method of presenting antibodies on the surface of LNPs using scFv that binds to the Fc domain of antibodies has been reported, which is called anchored secondary scFv enabling targeting (ASSET) by the authors [77]. Specifically, the scFv of RG7/1.30, a monoclonal antibody that binds to rat IgG2a, was linking to its N-terminus a short peptide NlpA motif consisting of 6 amino acids that received lipidation during its expression in *E. coli* [94,95], which in turn, supported its anchoring to the LNP membranes. This anti-rat IgG2a scFv, conjugated with lipidated NlpA motif peptide (a kind of lipoprotein) was expressed on the inner membrane of *E. coli* by using the appropriate signal peptide. The purified lipoprotein was mixed with cholesterol to form micelles. The micelles were mixed with siRNA-encapsulated LNPs having a lipid composition of DLin-MC3-DMA, DSPC, cholesterol, DMG-PEG, and DSPE-PEG (50/10.5/38/1.4/0.1 molar ratio) for 48 h at 4 °C for post-insertion, which allowed to generate a platform to produce LNPs with antibodies targeting any molecules. Antibody-modified LNPs were completed by attaching antibodies, which are more uniformly aligned to the preferred orientation compared to conventional amine coupling and other random chemical modifications. In fact, in the example of anti-CD34 antibody, the CD34 binding of LNPs evaluated by enzyme-linked immunosorbent assay (ELISA) was 4.5 times higher in this ASSET approach. In addition, the following secondary advantages were pointed out: reduced non-specific accumulation due to the masking of the Fc domain, and a reduction in the amounts of antibodies required by 2 orders of magnitude. In this paper, LNPs encapsulating Cy5-labeled siRNAs conjugated with monoclonal antibodies against eight different target molecules were generated. It was demonstrated using flow cytometry that they can be used to easily switch target cells for subtype targeting of leukocytes.

The therapeutic effects of leukocyte subtype-selective siRNA or mRNA delivery using this system have been demonstrated in mouse models of several types of diseases [77,78]. For example, in mice with dextran sodium sulfate (DSS)-induced colitis, a standard model of inflammatory bowel disease (IBD), using anti-Ly6C antibody-modified LNPs, TNF-α siRNAs were administered intravenously three times every other day, starting on the third day after DSS administration [77]. This resulted in a reduction of TNF-α levels in the colon by approximately one-third and a concomitant reduction of interleukin-6 (IL-6) levels to the same level as in non-inflamed mice, which greatly alleviated symptoms. Incidentally, Ly6c is a marker for mouse circulating monocytes and inflammatory tissue macrophages. Similarly, in xenograft mice models intravenously injected with mantle cell lymphoma cell line using anti-CD29 antibody-modified LNPs, siRNA against Polo-like Kinase 1 (*Plk1*) gene (an oncogene encoding a kinase essential for mitosis), was administered every 3 days starting 5 days after cancer cell administration, resulting in nearly doubling the survival time [77]. Furthermore, this system is also effective for mRNA delivery, and it has been demonstrated that anti-Ly6C antibody-modified LNPs can be used to produce foreign proteins selectively and efficiently in Ly6C-positive cells of spleen and intestine, using luciferase as a reporter [78]. In the same mouse model of IBD as above, the mRNA administration of IL-10 (one of the anti-inflammatory cytokines), with anti-Ly6C antibody-modified LNPs at 3, 6, and 9 days after induction of colitis, was reported to increase IL-10 concentrations in the colon to near normal levels. There were also associated decreases in colonic TNF-α and IL-6 concentrations and improvement in symptoms. This approach is complicated in that, it used recombinant lipoproteins expressed in *E. coli*, and there are concerns about their toxicities.

In the generation of LNPs targeting active form of $\alpha_4\beta_7$ integrin, LNPs were modified with antibody-like molecules by a slightly different strategy [79]. The LNPs with DSPE-PEG-maleimide, through which the rat IgG2a antibody RG7/1.3 reduced with dithiothreitol was conjugated, has been used in place of ASSET. For example, leukocytes are homing when $\alpha_4\beta_7$ integrin, which is expressed and activated on their membranes, attaches to MAdCAM-1 on intestinal endothelial cells. $\alpha_4\beta_7$ integrin undergoes a conformational change upon activation, and its natural ligand MAdCAM-1 is known to bind with higher affinity to this active form [96]. Therefore, the integrin-binding domain of MAdCAM-1 was fused to the rat IgG2a Fc, which was linked to the LNPs as a targeting element. As a therapeutic demonstration using this LNP in a mouse model of piroxicam-accelerated colitis, an interferon-siRNA was administered every other day starting 4 days after the start of piroxicam administration. The interferon concentration in the

colon decreased, and accordingly, colonic TNF-α and blood IL-6 and IL-1β concentrations decreased. The therapeutic outcome, improvement of colon pathologies, was also shown to be comparable to that of treatment with anti-TNF-α antibodies, which are already in standard use in clinical practice.

Although there are other reports of antibody modification of LNPs using maleimide-thiol coupling [80,81], the indirect modification approaches via the antibodies Fc domain binding molecule such as that described above are more versatile. Several other Fc domain binding molecules have been reported [97], among which peptidic ones may potentially be an alternative because their lipid conjugates can be chemically synthesized. Recent advances in mRNA display and other screening methods have made it possible to discover peptidic ligands from the libraries with a high degree of freedom in molecular design [98,99]. These include non-natural amino acids, and in some cases, the peptides with affinity and specificity greater than that of antibodies were reported to be obtained. Considering the stability of the formulations, it is expected that the development of LNPs with such peptidic ligands as targeting elements will be advanced in the future. We reviewed the successful examples of active targeting of LNPs with antibodies and other targeting elements. It is important to emphasize that these approaches do not fundamentally change tissue selectivity, but rather provide enhanced selectivity for cellular uptake in the tissues to which LNPs were distributed, leading to superior drug efficacy.

5. Application to gene editing therapy

With the emergence of clustered regularly interspaced short palindromic repeats (CRISPR) [100–102] as the third generation of editing technology following Zinc finger and TALEN [103,104], gene editing therapy is slowly becoming a reality [105,106]. There are three major types of CRISPR gene editing: non-homologous end joining (NHEJ), homology-directed repair (HDR), and base editing, each of which requires different components based on its mechanism (Fig. 4) [104,107]. Of these, NHEJ and HDR take advantage of the fact that the Cas 9 nuclease makes a double-strand break at specific locations in the genome targeted by single-guide RNAs (sgRNAs). Mutations are introduced during subsequent repair process, causing frameshifts and premature termination codons [104]. During this repair process, HDR occurs if there is a donor DNA (repair template) with the same homology arms as the adjacent sequences of the double-strand break site, or NHEJ due to a random insertion/deletion if there is no donor DNA [104]. In base editing, instead of Cas9, base editors, which are fusion proteins of a mutant dead Cas9 (dCas9) having inactivated DNA cleavage and cytidine or adenine deaminase, are used to replace C•G base pair to T•A base pair or vice versa without cleaving the DNA strand [107–109]. While NHEJ and HDR mainly focus on disrupting the expression of abnormal genes that cause disease, base editing is different, in that it normalizes the target gene sequences and normal protein production is expected.

Efficient and safe CRISPR/Cas9 gene editing using viruses is not easy because of the large size of Cas9 and concerns about increased off-target efficiency due to maintaining the editing system for a long period of time [110]. Following their success with siRNA and mRNA, LNPs are expected to be one of the promising delivery systems in gene editing [110–115]. For NHEJ, there are two types of LNPs: those that encapsulate Cas9 mRNA and sgRNA together [116–118], and those that encapsulate ribonucleoproteins (RNPs), which are complexes of Cas9 protein and sgRNA [119,120]. A representative demonstration of the former is the editing of the transthyretin (*Ttr*) gene in the liver of mice and rats, and the subsequent knockdown of its expression [116]. The composition of the LNPs used was generally standard for liver-targeting LNPs, including cholesterol, DSPC, and PEG2k-DMG, except for an original biodegradable ionizable lipid with a pKa of approximately 6.1. In addition, Cas9 mRNA and sgRNA were mixed in LNPs at a weight ratio of 1:1. Since the length of each is approximately 4500 and 100 nucleotides, the molar ratio of sgRNA was 45 times greater than

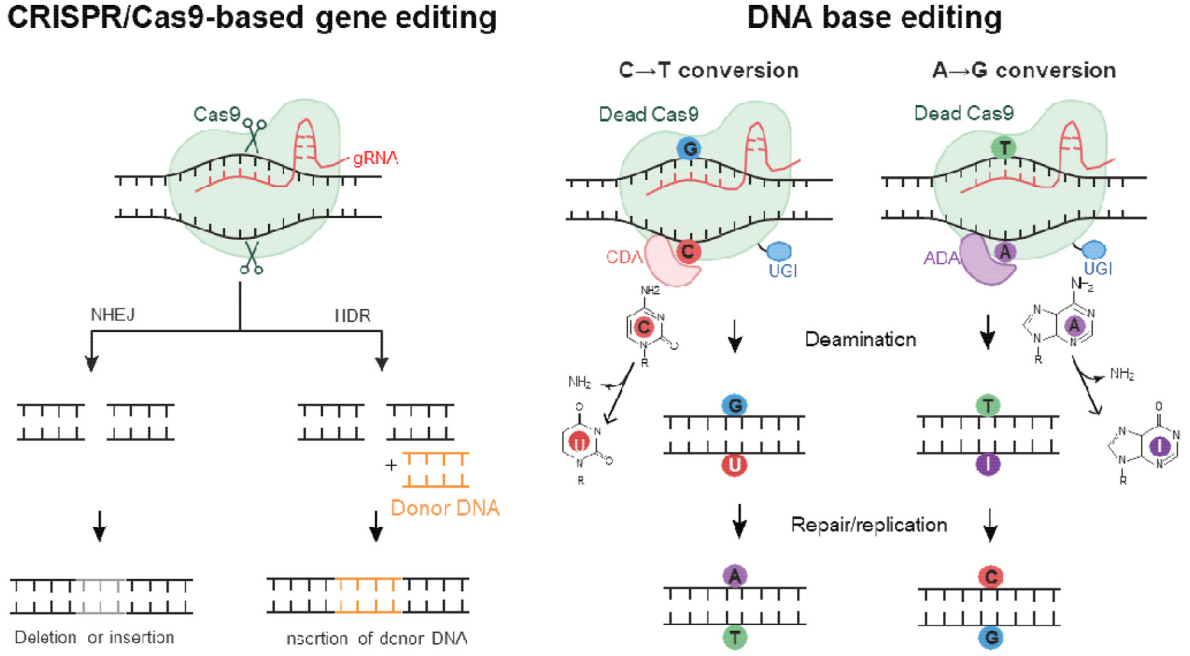

Fig. 4. The mechanisms of three types of CRISPR gene editing: non-homologous end joining (NHEJ), homology-directed repair (HDR), and base editing. The Cas9 nuclease makes a double-strand break at specific locations in the genome targeted by single-guide RNAs (sgRNAs). Mutations are introduced during subsequent repair process, causing frameshifts and premature termination codons. During the repair process, HDR occurs if there is a donor DNA, or NHEJ due to a random insertion/deletion if there is no donor DNA. In base editing, base editors, which are fusion proteins of a dead Cas9 and cytidine or adenine deaminase, are used to replace C•G base pair to T•A base pair or vice versa without cleaving the DNA strand.

that of Cas9 mRNA. Cas9 with a nuclear localization sequence attached to its C-terminus was used. Furthermore, for sgRNAs, the 2′-*O*-methylation of 5′-terminal trinucleotide and parts of CRISPR RNA and *trans*-activating CRISPR RNA moieties, combined with the phosphorothioation of three bonds at both of the 5′- and 3′-termini, were shown to dramatically improve the editing efficiency. This chemical modification is thought to contribute to the maintenance of sgRNAs until Cas9 is translated, and thus, to the efficient formation of Cas9/sgRNA RNPs. The particle sizes of the resulting LNPs were generally less than 100 nm with the PdI approximately 0.1, which was comparable to those of siRNA- or mRNA-encapsulated LNPs. A single intravenous administration of this LNP at 3 mg/kg was reported to result in editing of approximately 70% of the *Ttr* gene in the liver by 4 days, and persistent knockdown of more than 97% of serum TTR for more than 1 year. This approach has the potential to edit genes in almost all hepatocytes, which account for 50−60% of all liver cells, and holds great promise for the treatment of various genetic liver diseases including transthyretin-type familial amyloid polyneuropathy.

In addition, in the liver, knockdown by NHEJ gene editing of *PCSK9* and *Angptl3*, genes for proprotein convertase subtilisin/kexin type 9 and angiopoietin-like 3, which are involved in the regulation of blood lipoprotein levels, was reported [117,118]. High editing efficiencies have been achieved by using unique ionizable lipids selected based on screening. Notably, both used ionizable lipids and lipidoids that contain disulfide bonds [117,118], and in the report of *Angptl3* editing, DOPC, which has a quaternary amine headgroup and one degree of unsaturation in the tail carbon chain, was used as a helper lipid because it was more efficient in protein expression by mRNA delivery than DSPC or DOPE [118].

Gene editing with NHEJ is being attempted outside of the liver, for example, in tumors [121]. Editing of the Polo-like Kinase 1 (*Plk1*) gene, an oncogene encoding a kinase required for mitosis, and its anticancer effects were investigated [122]. Since this gene is rarely expressed in normal, non-dividing cells that have undergone final differentiation, it is expected that the editing of this gene in normal cells around cancer cells do not cause abnormalities in their function in most cases [123]. In this LNP, an ionizable amino lipid with dilinoleyl chain and tertiary amine head group was used with DSPC, cholesterol, DMG-PEG, and DSPE-PEG, which was selected by in vitro screening, with fluorescent protein gene editing in HEK293 cells as a reporter [121]. Incidentally, the use of the typical ionizable amino lipid DLin-MC3-DMA was reported not to result in any editing under the same conditions, even though it was efficiently taken up by the cells. In orthotopic brain transplantation model mice of aggressive glioblastoma, a single intracerebral administration of 0.05 mg/kg of this LNP has been demonstrated to edit 68% of the *Plk1* in cancer cells, thereby suppressing tumor proliferation and prolonging survival. For an intraperitoneal dissemination xenograft model of human ovarian cancer, gene editing by intraperitoneal administration of LNPs displaying an anti-hEGFR antibody by the ASSET approach described above has been investigated. While the parent unmodified LNPs showed almost no editing, a single administration of 0.75 mg/kg of this LNP edited about 80% of the *Plk1* in cancer cells, and after two administrations, there was a marked suppression of tumor growth and 80% increase in survival rate. Unfortunately, it is limited to local administration for now, but compared to siRNA-based knockdown, the number of administrations may be greatly reduced, and gene editing of metastatic cancer and other cancers by systemic administration may be one of the goals of future LNPs development.

Cas9/sgRNA RNPs can be encapsulated into LNPs by taking advantage of their anionic nature [119,120]. Some modification is, however, required from the general methods for nucleic acid therapeutics, because their molecular weights are large (approximately 200 kDa) and there are concerns about their denaturation due to pH change. In a pioneering report, a buffer of pH 5.2 was used to prepare LNPs, and the particle size of the resulting LNPs was somewhat large (approximately 300 nm), which only demonstrated the editing of fluorescent protein gene in vitro [119]. In a recent paper, a method was proposed, in which a cationic lipid such as DOTAP, which has a positive charge even in neutral pH conditions, was added to ionizable lipid, DOPE, cholesterol, and DMG-PEG to encapsulate Cas9/sgRNA RNPs with neutral buffer solutions in order to eliminate concerns about their denaturation [120]. It was shown that LNPs with particle sizes of less than 200 nm and PdIs of less than 0.2 could be prepared. Furthermore, this method was quite generalizable to various combinations of cationic lipids, ionizable lipids and neutral pH buffers. In this paper, some NHEJ-based editing in the liver and lungs by systemic administration combined with the abovementioned SORT technology, was demonstrated. As interesting applications, the simultaneous knockout of three tumor suppressor genes (*PTEN*, *P53*, and *RB1*) in the liver and the generation of their fusion protein by rearrangement of *Eml4* and *Alk* in the lung were shown to develop mouse models of cancer. As an example of therapeutic applications, three intravenous administrations of this LNP (2.5 mg/kg sgRNA for *PCSK9*, once a week) edited the *PCSK9* gene in the liver and reduced the serum PCSK9 concentration by approximately half. In addition, three injections of this LNP (1 mg/kg sgRNA to cause therapeutic exon skipping or reframing, once a week) into tibialis anterior muscle partly restored the reading frame in Duchenne muscular dystrophy mouse model, which restored the expression of functional dystrophin protein to 4.2% of normal mice.

HDR requires the presence of donor DNA (repair template), in addition to Cas9 and sgRNA, during the repair process after the double-strand break. In an early report, donor DNA and sgRNA were made to persist for a certain period of time using adeno-associated virus vectors, and only Cas9 mRNA was delivered by LNP to achieve HDR [124]. In contrast, the development of LNPs that encapsulated all three essential components (Cas9 mRNA, sgRNA, and donor DNA) is a more convenient, all-in-one approach [125]. The lipids used in LNPs were a unique ionizable dendrimer-based lipid, cholesterol, DOPE, and PEG-DMG; the sgRNAs were stabilized by phosphorothioate modifications and 2′-*O*-methylations at the 2−3 bases of 5′ and 3′ termini, which is similar to those for NHEJ mentioned above. The optimal ratio of mRNA:sgRNA:donor DNA was found to be approximately 2:1:3 by weight, and since the DNA donor used in this study was single strand and approximately 130 nucleotides in size, their molar ratio was approximately 1:20:60. This study was designed to use HEK293 cells stably expressing the Y66H mutant of GFP, which emit blue fluorescence when unedited, no fluorescence when NHEJ occurs, and green when HDR occurs, and the ratios of these three states were determined by flow cytometry. In vitro evaluations showed that as the total editing efficiency increased, NHEJ was more likely to occur, accounting for one-third to nearly half of the total editing efficiency. The optimized LNPs edited the genes of more than 91% of the cells, of which approximately 60% were HDR. In addition, in vivo evaluation showed that the direct injection of LNPs into HEK293 (Y66H) xenografts resulted in HDR editing in just over 20% of cells. There have been few reports of HDR using LNP so far, and the efficiencies were far from satisfactory. The authors of the above paper suggested that the low utilization efficiency of donor DNA during repair, that is its low concentration in the nucleus, may be a limiting factor for HDR [125], which is one of the major issues to be overcome in future. Although using double-stranded donor DNAs, the addition of Cas9 binding sequences (for example, 16 bp truncated Cas9 target sequences) has been reported to increase localization in the nucleus and HDR efficiencies [126], and this approach may be a solution.

Recently, a paper was published on the demonstration of base editing of *PCSK9* using LNPs in non-human primates, which is one of the major milestones toward clinical applications [127]. In this paper, the adenine base editor 8.8-m (ABE8.8), which fused an evolved deoxyadenosine deaminase domain to the N-terminus of the core *Streptococcus pyogenes* nickase Cas9 and a bipartite nuclear localization sequence to the C-terminus [128], was used. The length of the ABE8.8 mRNA was approximately 5300 nucleotides, and it was encapsulated in LNPs along with PCSK9-1 sgRNA at a weight ratio of 1:1. The PCSK9-1 sgRNA used, targeted the splice donor at the boundary between exon 1 and intron 1 of *PCSK9*, and was designed so that the disruption of the splice donor led to read-through into the intron and its translation was stopped by the termination codon that exists immediately inside the intron. The single intravenous administration of this LNP at a dose of 1.0−3.0 mg/kg resulted in base-editing of more than 60% of *PCSK9* in the liver of cynomolgus monkeys, and a decrease in blood levels of PCSK9 and low-density lipoprotein cholesterol by approximately 80−90%, and 60%, respectively. In addition, these reductions were sustained for at least 8 months. It is noteworthy that the rates of insertion or deletion mutations were less than 0.5%, and off-target base editing was less than 1% at only one site. Incidentally, it was reported that base editing occurred in a similar manner in cultured human primary hepatocytes with no discernible off-targeting editing. Another paper with a very similar study design was reported by another group at about the same time, in which antibodies against Cas9 and deaminase were found to be produced one month after LNP administration, and it was argued that this might affect the editing efficiency of the second administration [129].

Cytidine base editing using LNPs was also demonstrated in Pah^{enu2} mouse model for phenylketonuria [130]. *Staphylococcus aureus* (*Sa*) KKH-CBE3 [131] was used as the base editor, and its mRNA and sgRNA for restoration of mutated Pah^{enu2} were encapsulated in general LNPs and administered intravenously at a dose of 3 mg/kg twice with weekly intervals. The on-target C-to-T conversion rate and the editing efficiency to wild-type phenylalanine hydroxylase sequences in the liver were around 10% and 5%, respectively, after the first dose, and around 20% and 10%, respectively, after the second dose. As a result, after the second dose, the L-Phe concentration in the blood decreased to below 360 μmol/L, which is the therapeutic threshold. In this study, the authors specifically focused on whether off-target editing occurs and reported that high-throughput sequencing of 10 predicted off-target loci, as well as whole genome sequencing, did not detect any off-target deamination. Base editing has advantages over NHEJ in terms of low insertion or deletion mutations and off-target editing frequency, and is simpler than HDR. These advantages should accelerate the development of base editing for clinical use.

More recently, RNA-targeted CRISPR-Cas systems were discovered [132−134], and it is worth mentioning that one of them, Cas13a, has started to be investigated for the treatment of RNA virus infections, especially during the current COVID-19 pandemic. Although the delivery was not by LNPs, but by polymers, it was demonstrated that Cas13a mRNA and CRISPR RNAs optimized for each virus could be administered through the respiratory tract using a nebulizer to efficiently degrade influenza RNA in the lung tissue of influenza-infected mice. They could also reduce SARS-CoV-2 virus replication and symptoms in hamsters receiving them 20 h prior to infection [135].

6. Summary and future scope

LNPs for nucleic acid, mRNA, and gene editing-based therapeutics are among the first successful examples of bringing a full-fledged screening-based approach to the field of DDS development. It has an affinity for the drug development process of pharmaceutical companies and is expected to lead to DDS-oriented drug development, which is the need of the hour. From now on, LNP research and development will focus on addressing the following: expanding the scope of drug delivery to different constituents of the human body, expanding the number of diseases that can be targeted, and studying the change in the pharmacokinetics of LNPs under pathological conditions.

Just as patisiran (Onpattro) targets for transthyretin-type familial amyloid polyneuropathy, the current approach using standard formulations of LNPs will be smoothly applied to nucleic acid, mRNA, and gene editing-based therapeutics, especially for rare hepatic genetic diseases for which no treatment exists. In addition, recently, attempts to treat cancers by neutralizing antibody production in the liver [136−139] and by administrations of multiple mRNAs have begun to be demonstrated using rodents [140,141]. For example, intravenous administration of LNPs with mRNA encoding bi-specific single-domain antibodies to the chemokines CCL2 and CCL5, was reported to convert TAMs from M2 to M1 phenotype, thereby suppressing immune tolerance; and in combination with PD-1 ligand inhibitor, to prolong the survival durations of mouse models of liver cancer and liver metastasis [139]. Intratumoral administration of LNPs encapsulating three types of mRNAs encoding IL-23, IL-36 and OX40L, has been shown to be effective in recruiting immune cells, destroying tumors, and prolonging survival durations in syngeneic models of mouse colon cancers [140]. Another study included the treatment of propionic acidemia/aciduria with LNPs containing two mRNAs, encoding the genes for the mitochondrial enzymes propionyl-CoA carboxylase subunit alpha (PCCA) and PCC subunit beta (PCCB) [141]. Also, aimed at application in prenatal therapy, it was demonstrated using erythropoietin as an example that vitelline vein injection of the LNP formulations were able to deliver mRNAs in mice, mainly to the livers of the fetuses for production of therapeutic proteins [142].

Physiological and pathological factors that may affect delivery and subsequent protein expression have also begun to be investigated in mice. Mild TLR4 activation by moderate doses of LPS, suppressed the translation of mRNA delivered by LNPs in hepatocytes, liver endothelial cells, and Kupffer cells, which was suggested to be due to the involvement of reduction in endosomal escape and mRNA translation, rather than reduced uptake of LNPs [143]. It has been proposed that inhibition of TLR4 or protein kinase R, may restore mRNA translation, and this may be one of the points to be considered in the development of mRNA/LNPs for inflammation-related diseases such as myocardial infarction and colitis [143]. In addition, it was shown that an increase in basal metabolism induced by phosphatidylinositol (3,4,5)-trisphosphate (PIP3) significantly suppressed the production of foreign proteins by mRNA/LNPs in lung endothelial cells, spleen endothelial cells, and hepatocytes. The reasons for this have been proposed to be the depletion of intracellular resources by over-consumption, the enhanced protein degradation, or inhibited transcription [144]. Thus, it has been suggested that the metabolic states of the cells may be a factor that greatly affects the success or failure of LNP-mediated nucleic acid, mRNA, and gene editing therapeutics. It would be a useful approach to explore the drug combinations that lead to the acceleration of mRNA delivery and translation, as was the original aim of this study.

With future advances, we hope that the development of nucleic acids, mRNA, and gene editing-based therapeutics based on this LNP technology will become one of the golden standards for drug development for a wide range of diseases, leading to reduced development costs and shorter development times.

Author contributions

H.M., K.O., N.K., and S.K. contributed to the writing, reviewing and editing of the manuscript.

Declaration of competing interest

The authors declare no conflicts of interest associated with this manuscript.

Acknowledgements

This study was supported, in part, by JSPS KAKENHI (Grant 21H03818) and the Project for Cancer Research and Therapeutic Evolution (P-CREATE) of the Japan Agency for Medical Research and Development (AMED) (Grant JP21cm0106201).

References

[1] Cullis PR, Hope MJ. Lipid nanoparticle systems for enabling gene therapies. Mol Ther 2017;25(7):1467–75.
[2] Hou X, Zaks T, Langer R, Dong Y. Lipid nanoparticles for mRNA delivery. Nat Rev Mater 2021:1–17.
[3] Kulkarni JA, Witzigmann D, Chen S, Cullis PR, Van Der Meel R. Lipid nanoparticle technology for clinical translation of siRNA therapeutics. Acc Chem Res 2019;52(9):2435–44.
[4] Samaridou E, Heyes J, Lutwyche P. Lipid nanoparticles for nucleic acid delivery: current perspectives. Adv Drug Deliv Rev 2020;154–155:37–63.
[5] Hu B, Zhong L, Weng Y, Peng L, Huang Y, Zhao Y, et al. Therapeutic siRNA: state of the art. Signal Transduct Target Ther 2020;5(1):101.
[6] Shin MD, Shukla S, Chung YH, Beiss V, Chan SK, Ortega-Rivera OA, et al. COVID-19 vaccine development and a potential nanomaterial path forward. Nat Nanotechnol 2020;15(8):646–55.
[7] Gebre MS, Brito LA, Tostanoski LH, Edwards DK, Carfi A, Barouch DH. Novel approaches for vaccine development. Cell 2021;184(6):1589–603.
[8] Witzigmann D, Kulkarni JA, Leung J, Chen S, Cullis PR, van der Meel R. Lipid nanoparticle technology for therapeutic gene regulation in the liver. Adv Drug Deliv Rev 2020;159:344–63.
[9] Kowalski PS, Rudra A, Miao L, Anderson DG. Delivering the messenger: advances in technologies for therapeutic mRNA delivery. Mol Ther 2019;27(4):710–28.
[10] Schoenmaker L, Witzigmann D, Kulkarni JA, Verbeke R, Kersten G, Jiskoot W, et al. mRNA-lipid nanoparticle COVID-19 vaccines: structure and stability. Int J Pharm 2021;601:120586.
[11] Semple SC, Akinc A, Chen J, Sandhu AP, Mui BL, Cho CK, et al. Rational design of cationic lipids for siRNA delivery. Nat Biotechnol 2010;28(2):172–6.
[12] Rietwyk S, Peer D. Next-generation lipids in RNA interference therapeutics. ACS Nano 2017;11(8):7572–86.
[13] Patel P, Ibrahim NM, Cheng K. The importance of apparent pKa in the development of nanoparticles encapsulating siRNA and mRNA. Trends Pharmacol Sci 2021;42(6):448–60.
[14] Jayaraman M, Ansell SM, Mui BL, Tam YK, Chen J, Du X, et al. Maximizing the potency of siRNA lipid nanoparticles for hepatic gene silencing in vivo. Angew Chem Int Ed Engl 2012;51(34):8529–33.
[15] Hassett KJ, Benenato KE, Jacquinet E, Lee A, Woods A, Yuzhakov O, et al. Optimization of lipid nanoparticles for intramuscular administration of mRNA vaccines. Mol Ther Nucleic Acids 2019;15:1–11.
[16] Akita H, Ishiba R, Hatakeyama H, Tanaka H, Sato Y, Tange K, et al. A neutral envelope-type nanoparticle containing pH-responsive and ss-cleavable lipid-like material as a carrier for plasmid DNA. Adv Healthc Mater 2013;2(8):1120–5.
[17] Tanaka H, Sakurai Y, Anindita J, Akita H. Development of lipid-like materials for RNA delivery based on intracellular environment-responsive membrane destabilization and spontaneous collapse. Adv Drug Deliv Rev 2020;154–155:210–26.
[18] Love KT, Mahon KP, Levins CG, Whitehead KA, Querbes W, Dorkin JR, et al. Lipid-like materials for low-dose, in vivo gene silencing. Proc Natl Acad Sci USA 2010;107(5):1864–9.
[19] Leuschner F, Dutta P, Gorbatov R, Novobrantseva TI, Donahoe JS, Courties G, et al. Therapeutic siRNA silencing in inflammatory monocytes in mice. Nat Biotechnol 2011;29(11):1005–10.
[20] Kauffman KJ, Dorkin JR, Yang JH, Heartlein MW, Derosa F, Mir FF, et al. Optimization of lipid nanoparticle formulations for mRNA delivery in vivo with fractional factorial and definitive screening designs. Nano Lett 2015;15(11):7300–6.
[21] Hatakeyama H, Akita H, Harashima H. A multifunctional envelope type nano device (MEND) for gene delivery to tumours based on the EPR effect: a strategy for overcoming the PEG dilemma. Adv Drug Deliv Rev 2011;63(3):152–60.
[22] Hatakeyama H, Akita H, Harashima H. The polyethyleneglycol dilemma: advantage and disadvantage of PEGylation of liposomes for systemic genes and nucleic acids delivery to tumors. Biol Pharm Bull 2013;36(6):892–9.
[23] Sun Q, Zhou Z, Qiu N, Shen Y. Rational design of cancer nanomedicine: nanoproperty integration and synchronization. Adv Mater 2017;29(14):1606628.
[24] Mui BL, Tam YK, Jayaraman M, Ansell SM, Du X, Lin PJC, et al. Influence of polyethylene glycol lipid desorption rates on pharmacokinetics and pharmacodynamics of siRNA lipid nanoparticles. Mol Ther Nucleic Acids 2013;2(12):e139.
[25] Akinc A, Maier MA, Manoharan M, Fitzgerald K, Jayaraman M, Barros S, et al. The Onpattro story and the clinical translation of nanomedicines containing nucleic acid-based drugs. Nat Nanotechnol 2019;14(12):1084–7.
[26] Ramaswamy S, Tonnu N, Tachikawa K, Limphong P, Vega JB, Karmali PP, et al. Systemic delivery of factor IX messenger RNA for protein replacement therapy. Proc Natl Acad Sci USA 2017;114(10):E1941–50.
[27] Belliveau NM, Huft J, Lin PJ, Chen S, Leung AK, Leaver TJ, et al. Microfluidic synthesis of highly potent limit-size lipid nanoparticles for in vivo delivery of siRNA. Mol Ther Nucleic Acids 2012;1(8):e37.
[28] Zhigaltsev IV, Belliveau N, Hafez I, Leung AKK, Huft J, Hansen C, et al. Bottom-up design and synthesis of limit size lipid nanoparticle systems with aqueous and triglyceride cores using millisecond microfluidic mixing. Langmuir 2012;28(7):3633–40.
[29] Maeki M, Kimura N, Sato Y, Harashima H, Tokeshi M. Advances in microfluidics for lipid nanoparticles and extracellular vesicles and applications in drug delivery systems. Adv Drug Deliv Rev 2018;128:84–100.
[30] Arteta MY, Kjellman T, Bartesaghi S, Wallin S, Wu X, Kvist AJ, et al. Successful reprogramming of cellular protein production through mRNA delivered by functionalized lipid nanoparticles. Proc Natl Acad Sci USA 2018;115(15):E3351–60.
[31] Viger-Gravel J, Schantz A, Pinon AC, Rossini AJ, Schantz S, Emsley L. Structure of lipid nanoparticles containing siRNA or mRNA by dynamic nuclear polarization-enhanced NMR spectroscopy. J Phys Chem B 2018;122(7):2073–81.
[32] Leung AKK, Hafez IM, Baoukina S, Belliveau NM, Zhigaltsev IV, Afshinmanesh E, et al. Lipid nanoparticles containing siRNA synthesized by microfluidic mixing exhibit an electron-dense nanostructured core. J Phys Chem C Nanomater Interfaces 2012;116(34):18440–50.
[33] Massoud TF, Gambhir SS. Molecular imaging in living subjects: seeing fundamental biological processes in a new light. Genes Dev 2003;17(5):545–80.
[34] Pardi N, Tuyishime S, Muramatsu H, Kariko K, Mui BL, Tam YK, et al. Expression kinetics of nucleoside-modified mRNA delivered in lipid nanoparticles to mice by various routes. J Contr Release 2015;217:345–51.
[35] Zhang N, Li X, Deng Y, Zhao H, Huang Y, Yang G, et al. A Thermostable mRNA vaccine against COVID-19. Cell 2020;182(5):1271–83. e16.
[36] Kuchimaru T, Iwano S, Kiyama M, Mitsumata S, Kadonosono T, Niwa H, et al. A luciferin analogue generating near-infrared bioluminescence achieves highly sensitive deep-tissue imaging. Nat Commun 2016;7:11856.
[37] Iwano S, Sugiyama M, Hama H, Watakabe A, Hasegawa N, Kuchimaru T, et al. Single-cell bioluminescence imaging of deep tissue in freely moving animals. Science 2018;359(6378):935–9.
[38] Akinc A, Querbes W, De S, Qin J, Frank-Kamenetsky M, Jayaprakash KN, et al. Targeted delivery of RNAi therapeutics with endogenous and exogenous ligand-based mechanisms. Mol Ther 2010;18(7):1357–64.
[39] Sakurai F, Nishioka T, Saito H, Baba T, Okuda A, Matsumoto O, et al. Interaction between DNA-cationic liposome complexes and erythrocytes is an important factor in systemic gene transfer via the intravenous route in mice: the role of the neutral helper lipid. Gene Ther 2001;8(9):677–86.
[40] Sakurai F, Nishioka T, Yamashita F, Takakura Y, Hashida M. Effects of erythrocytes and serum proteins on lung accumulation of lipoplexes containing cholesterol or DOPE as a helper lipid in the single-pass rat lung perfusion system. Eur J Pharm Biopharm 2001;52(2):165–72.
[41] Opanasopit P, Nishikawa M, Hashida M. Factors affecting drug and gene delivery: effects of interaction with blood components. Crit Rev Ther Drug Carrier Syst 2002;19(3):191–233.
[42] Chen D, Ganesh S, Wang W, Amiji M. The role of surface chemistry in serum protein corona-mediated cellular delivery and gene silencing with lipid nanoparticles. Nanoscale 2019;11(18):8760–75.
[43] Chen D, Parayath N, Ganesh S, Wang W, Amiji M. The role of apolipoprotein-and vitronectin-enriched protein corona on lipid nanoparticles for- and vivo targeted delivery and transfection of oligonucleotides in murine tumor models. Nanoscale 2019;11(40):18806–24.
[44] Sebastiani F, Yanez Arteta M, Lerche M, Porcar L, Lang C, Bragg RA, et al. Apolipoprotein E binding drives structural and compositional rearrangement of mRNA-containing lipid nanoparticles. ACS Nano 2021;15(4):6709–22.
[45] Sato Y, Kinami Y, Hashiba K, Harashima H. Different kinetics for the hepatic uptake of lipid nanoparticles between the apolipoprotein E/low density lipoprotein receptor and the N-acetyl-D-galactosamine/asialoglycoprotein receptor pathway. J Contr Release 2020;322:217–26.
[46] Francia V, Schiffelers RM, Cullis PR, Witzigmann D. The biomolecular corona of lipid nanoparticles for gene therapy. Bioconjugate Chem 2020;31(9):2046–59.
[47] Cheng Q, Wei T, Farbiak L, Johnson LT, Dilliard SA, Siegwart DJ. Selective organ targeting (SORT) nanoparticles for tissue-specific mRNA delivery and CRISPR–Cas gene editing. Nat Nanotechnol 2020;15(4):313–20.

[48] Ma F, Yang L, Sun Z, Chen J, Rui X, Glass Z, et al. Neurotransmitter-derived lipidoids (NT-lipidoids) for enhanced brain delivery through intravenous injection. Sci Adv 2020;6(30):eabb4429.
[49] Kim M, Jeong M, Hur S, Cho Y, Park J, Jung H, et al. Engineered ionizable lipid nanoparticles for targeted delivery of RNA therapeutics into different types of cells in the liver. Sci Adv 2021;7(9):eabf4398.
[50] Madisen L, Zwingman TA, Sunkin SM, Oh SW, Zariwala HA, Gu H, et al. A robust and high-throughput Cre reporting and characterization system for the whole mouse brain. Nat Neurosci 2010;13(1):133–40.
[51] Kretzschmar K, Watt FM. Lineage tracing. Cell 2012;148(1–2):33–45.
[52] Josh Huang Z, Zeng H. Genetic approaches to neural circuits in the mouse. Annu Rev Neurosci 2013;36:183–215.
[53] Gupta N, Price PM, Aboagye EO. PET for in vivo pharmacokinetic and pharmacodynamic measurements. Eur J Cancer 2002;38(16):2094–107.
[54] Sugiyama Y, Yamashita S. Impact of microdosing clinical study - why necessary and how useful? Adv Drug Deliv Rev 2011;63(7):494–502.
[55] Bergström M, Grahnén A, Långström B. Positron emission tomography microdosing: a new concept with application in tracer and early clinical drug development. Eur J Clin Pharmacol 2003;59(5–6):357–66.
[56] Yamashita S, Takashima T, Kataoka M, Oh H, Sakuma S, Takahashi M, et al. PET imaging of the gastrointestinal absorption of orally administered drugs in conscious and anesthetized rats. J Nucl Med 2011;52(2):249–56.
[57] Takashima T, Yokoyama C, Mizuma H, Yamanaka H, Wada Y, Onoe K, et al. Developmental changes in P-glycoprotein function in the blood-brain barrier of nonhuman primates: PET study with R-^{11}C-verapamil and ^{11}C-oseltamivir. J Nucl Med 2011;52(6):950–7.
[58] Wei W, Rosenkrans ZT, Liu J, Huang G, Luo Q, Cai W. ImmunoPET: concept, design, and applications. Chem Rev 2020;120(8):3787–851.
[59] Sakai K, Passioura T, Sato H, Ito K, Furuhashi H, Umitsu M, et al. Macrocyclic peptide-based inhibition and imaging of hepatocyte growth factor. Nat Chem Biol 2019;15(6):598–606.
[60] Ren Q, Mohri K, Warashina S, Wada Y, Watanabe Y, Mukai H. Improved immuno-PET imaging of HER2-positive tumors in mice: urokinase injection-triggered clearance enhancement of 64Cu-trastuzumab. Mol Pharm 2019;16(3):1065–73.
[61] Mukai H, Watanabe Y. Review: PET imaging with macro- and middle-sized molecular probes. Nucl Med Biol 2021;92:156–70.
[62] Tavitian B, Terrazzino S, Kühnast B, Marzabal S, Stettler O, Dollé F, et al. In vivo imaging of oligonucleotides with positron emission tomography. Nat Med 1998;4(4):467–71.
[63] Kuboyama T, Nakahara M, Yoshino M, Cui Y, Sako T, Wada Y, et al. Stoichiometry-focused ^{18}F-labeling of alkyne-substituted oligodeoxynucleotides using azido([^{18}F]fluoromethyl)benzenes by Cu-catalyzed Huisgen reaction. Bioorg Med Chem 2011;19(1):249–55.
[64] Mukai H, Ozaki D, Cui Y, Kuboyama T, Yamato-Nagata H, Onoe K, et al. Quantitative evaluation of the improvement in the pharmacokinetics of a nucleic acid drug delivery system by dynamic PET imaging with ^{18}F-incorporated oligodeoxynucleotides. J Contr Release 2014;180:92–9.
[65] Mukai H, Hatanaka K, Yagi N, Warashina S, Zouda M, Takahashi M, et al. Pharmacokinetic evaluation of liposomal nanoparticle-encapsulated nucleic acid drug: a combined study of dynamic PET imaging and LC/MS/MS analysis. J Contr Release 2019;294:185–94.
[66] Lindsay KE, Bhosle SM, Zurla C, Beyersdorf J, Rogers KA, Vanover D, et al. Visualization of early events in mRNA vaccine delivery in non-human primates via PET–CT and near-infrared imaging. Nat Biomed Eng 2019;3(5):371–80.
[67] Dahlman JE, Kauffman KJ, Xing Y, Shaw TE, Mir FF, Dlott CC, et al. Barcoded nanoparticles for high throughput in vivo discovery of targeted therapeutics. Proc Natl Acad Sci USA 2017;114(8):2060–5.
[68] Lokugamage MP, Sago CD, Dahlman JE. Testing thousands of nanoparticles in vivo using DNA barcodes. Curr Opin Biomed Eng 2018;7:1–8.
[69] Zhang R, El-Mayta R, Murdoch TJ, Warzecha CC, Billingsley MM, Shepherd SJ, et al. Helper lipid structure influences protein adsorption and delivery of lipid nanoparticles to spleen and liver. Biomater Sci 2021;9(4):1449–63.
[70] Guimaraes PPG, Zhang R, Spektor R, Tan M, Chung A, Billingsley MM, et al. Ionizable lipid nanoparticles encapsulating barcoded mRNA for accelerated in vivo delivery screening. J Contr Release 2019;316:404–17.
[71] Paunovska K, Da Silva Sanchez AJ, Sago CD, Gan Z, Lokugamage MP, Islam FZ, et al. Nanoparticles containing oxidized cholesterol deliver mRNA to the liver microenvironment at clinically relevant doses. Adv Mater 2019;31(14):e1807748.
[72] Sago CD, Lokugamage MP, Lando GN, Djeddar N, Shah NN, Syed C, et al. Modifying a commonly expressed endocytic receptor retargets nanoparticles in vivo. Nano Lett 2018;18(12):7590–600.
[73] Schoch CL, Seifert KA, Huhndorf S, Robert V, Spouge JL, Levesque CA, et al. Nuclear ribosomal internal transcribed spacer (ITS) region as a universal DNA barcode marker for Fungi. Proc Natl Acad Sci USA 2012;109(16):6241–6.
[74] Kress WJ, Wurdack KJ, Zimmer EA, Weigt LA, Janzen DH. Use of DNA barcodes to identify flowering plants. Proc Natl Acad Sci USA 2005;102(23):8369–74.
[75] Hindson BJ, Ness KD, Masquelier DA, Belgrader P, Heredia NJ, Makarewicz AJ, et al. High-throughput droplet digital PCR system for absolute quantitation of DNA copy number. Anal Chem 2011;83(22):8604–10.
[76] Goswami R, Chatzikleanthous D, Lou G, Giusti F, Bonci A, Taccone M, et al. Mannosylation of LNP results in improved potency for self-amplifying RNA (SAM) vaccines. ACS Infect Dis 2019;5(9):1546–58.
[77] Kedmi R, Veiga N, Ramishetti S, Goldsmith M, Rosenblum D, Dammes N, et al. A modular platform for targeted RNAi therapeutics. Nat Nanotechnol 2018;13(3):214–9.
[78] Veiga N, Goldsmith M, Granot Y, Rosenblum D, Dammes N, Kedmi R, et al. Cell specific delivery of modified mRNA expressing therapeutic proteins to leukocytes. Nat Commun 2018;9(1):4493.
[79] Dammes N, Goldsmith M, Ramishetti S, Dearling JLJ, Veiga N, Packard AB, et al. Conformation-sensitive targeting of lipid nanoparticles for RNA therapeutics. Nat Nanotechnol 2021;16(9):1030–8.
[80] Ramishetti S, Hazan-Halevy I, Palakuri R, Chatterjee S, Gonna SN, Dammes N, et al. A combinatorial library of lipid nanoparticles for RNA delivery to leukocytes. Adv Mater 2020;32(12):e1906128.
[81] Ramishetti S, Kedmi R, Goldsmith M, Leonard F, Sprague AG, Godin B, et al. Systemic gene silencing in primary T lymphocytes using targeted lipid nanoparticles. ACS Nano 2015;9(7):6706–16.
[82] Li S, Huang L. Pharmacokinetics and biodistribution of nanoparticles. Mol Pharm 2008;5(4):496–504.
[83] Levchenko TS, Rammohan R, Lukyanov AN, Whiteman KR, Torchilin VP. Liposome clearance in mice: the effect of a separate and combined presence of surface charge and polymer coating. Int J Pharm 2002;240(1–2):95–102.
[84] Hashida M, Kawakami S, Yamashita F. Lipid carrier systems for targeted drug and gene delivery. Chem Pharm Bull 2005;53(8):871–80.
[85] Kawakami S, Sato A, Nishikawa M, Yamashita F, Hashida M. Mannose receptor-mediated gene transfer into macrophages using novel mannosylated cationic liposomes. Gene Ther 2000;7(4):292–9.
[86] Kawakami S, Nishikawa M, Yamashita F, Hashida M. In vivo gene delivery to the liver using novel galactosylated cationic liposomes. Pharm Res (N Y) 2000;17(3):306–13.
[87] Kawakami S, Hashida M. Glycosylation-mediated targeting of carriers. J Contr Release 2014;190:542–55.
[88] Kawakami S, Higuchi Y, Hashida M. Nonviral approaches for targeted delivery of plasmid DNA and oligonucleotide. J Pharmacol Sci 2008;97(2):726–45.
[89] Jain K, Kesharwani P, Gupta U, Jain NK. A review of glycosylated carriers for drug delivery. Biomaterials 2012;33(16):4166–86.
[90] Linehan SA, Martínez-Pomares L, Stahl PD, Gordon S. Mannose receptor and its putative ligands in normal murine lymphoid and nonlymphoid organs: in situ expression of mannose receptor by selected macrophages, endothelial cells, perivascular microglia, and mesangial cells, but not dendritic cells. J Exp Med 1999;189(12):1961–72.
[91] Park JW, Hong K, Kirpotin DB, Colbern G, Shalaby R, Baselga J, et al. Anti-HER2 immunoliposomes: enhanced efficacy attributable to targeted delivery. Clin Cancer Res 2002;8(4):1172–81.
[92] Maruyama K, Kennel SJ, Huang L. Lipid composition is important for highly efficient target binding and retention of immunoliposomes. Proc Natl Acad Sci USA 1990;87(15):5744–8.
[93] Maruyama K, Ishida O, Takizawa T, Moribe K. Possibility of active targeting to tumor tissues with liposomes. Adv Drug Deliv Rev 1999;40(1–2):89–102.
[94] Yamaguchi K, Yu F, Inouye M. A single amino acid determinant of the membrane localization of lipoproteins in E. coli. Cell 1988;53(3):423–32.
[95] Harvey BR, Georgiou G, Hayhurst A, Jeong KJ, Iverson BL, Rogers GK. Anchored periplasmic expression, a versatile technology for the isolation of high-affinity antibodies from Escherichia coli-expressed libraries. Proc Natl Acad Sci USA 2004;101(25):9193–8.
[96] Berlin C, Berg EL, Briskin MJ, Andrew DP, Kilshaw PJ, Holzmann B, et al. α4β7 integrin mediates lymphocyte binding to the mucosal vascular addressin MAdCAM-1. Cell 1993;74(1):185–95.
[97] Choe W, Durgannavar TA, Chung SJ. Fc-binding ligands of immunoglobulin G: an overview of high affinity proteins and peptides. Materials 2016;9(12):994.
[98] Passioura T, Katoh T, Goto Y, Suga H. Selection-based discovery of druglike macrocyclic peptides. Annu Rev Biochem 2014;83:727–52.
[99] Josephson K, Ricardo A, Szostak JW. mRNA display: from basic principles to macrocycle drug discovery. Drug Discov Today 2014;19(4):388–99.
[100] Doudna J, Charpentier E. Genome editing. The new frontier of genome engineering with CRISPR-Cas9. Science 2014;346(6213):1258096.
[101] Cong L, Ran FA, Cox D, Lin S, Barretto R, Habib N, et al. Multiplex genome engineering using CRISPR/Cas systems. Science 2013;339(6121):819–23.
[102] Mali P, Yang L, Esvelt KM, Aach J, Guell M, DiCarlo JE, et al. RNA-guided human genome engineering via Cas9. Science 2013;339(6121):823–6.
[103] Gaj T, Gersbach CA, Barbas CF. ZFN, TALEN, and CRISPR/Cas-based methods for genome engineering. Trends Biotechnol 2013;31(7):397–405.
[104] Ran FA, Hsu PD, Wright J, Agarwala V, Scott DA, Zhang F. Genome engineering using the CRISPR-Cas9 system. Nat Protoc 2013;8(11):2281–308.
[105] Maeder M, Stefanidakis M, Wilson CJ, Baral R, Barrera LA, Bounoutas GS, et al. Development of a gene-editing approach to restore vision loss in Leber congenital amaurosis type 10. Nat Med 2019;25(2):229–33.
[106] Knott GJ, Doudna JA. CRISPR-Cas guides the future of genetic engineering. Science 2018;361(6405):866–9.
[107] Rees H, Liu DR. Base editing: precision chemistry on the genome and transcriptome of living cells. Nat Rev Genet 2018;19(12):770–88.

[108] Komor AC, Kim YB, Packer MS, Zuris JA, Liu DR. Programmable editing of a target base in genomic DNA without double-stranded DNA cleavage. Nature 2016;533(7603):420–4.
[109] Nishida K, Arazoe T, Yachie N, Banno S, Kakimoto M, Tabata M, et al. Targeted nucleotide editing using hybrid prokaryotic and vertebrate adaptive immune systems. Science 2016;353(6305):aaf8729.
[110] Yin H, Kauffman KJ, Anderson DG. Delivery technologies for genome editing. Nat Rev Drug Discov 2017;16(6):387–99.
[111] van Haasteren J, Li J, Scheideler OJ, Murthy N, Schaffer DV. The delivery challenge: fulfilling the promise of therapeutic genome editing. Nat Biotechnol 2020;38(7):845–55.
[112] Lino CA, Harper JC, Carney JP, Timlin JA. Delivering crispr: a review of the challenges and approaches. Drug Deliv 2018;25(1):1234–57.
[113] Liu C, Zhang L, Liu H, Cheng K. Delivery strategies of the CRISPR-Cas9 gene-editing system for therapeutic applications. J Contr Release 2017;266:17–26.
[114] Mashel TV, Tarakanchikova YV, Muslimov AR, Zyuzin MV, Timin AS, Lepik KV, et al. Overcoming the delivery problem for therapeutic genome editing: current status and perspective of non-viral methods. Biomaterials 2020;258:120282.
[115] Xu C, Chen G, Luo Y, Zhang Y, Zhao G, Lu Z, et al. Rational designs of in vivo CRISPR-Cas delivery systems. Adv Drug Deliv Rev 2021;168:3–29.
[116] Finn JD, Smith AR, Patel MC, Shaw L, Youniss MR, van Heteren J, et al. A single administration of CRISPR/Cas9 lipid nanoparticles achieves robust and persistent in vivo genome editing. Cell Rep 2018;22(9):2227–35.
[117] Liu J, Chang J, Jiang Y, Meng X, Sun T, Mao L, et al. Fast and efficient CRISPR/Cas9 genome editing in vivo enabled by bioreducible lipid and messenger RNA nanoparticles. Adv Mater 2019;31(33):e1902575.
[118] Qiu M, Glass Z, Chen J, Haas M, Jin X, Zhao X, et al. Lipid nanoparticle-mediated codelivery of Cas9 mRNA and single-guide RNA achieves liver-specific in vivo genome editing of Angptl3. Proc Natl Acad Sci USA 2021;118(10):e2020401118.
[119] Wang M, Zuris JA, Meng F, Rees H, Sun S, Deng P, et al. Efficient delivery of genome-editing proteins using bioreducible lipid nanoparticles. Proc Natl Acad Sci U S A 2016;113(11):2868–73.
[120] Wei T, Cheng Q, Min Y, Olson EN, Siegwart DJ. Systemic nanoparticle delivery of CRISPR-Cas9 ribonucleoproteins for effective tissue specific genome editing. Nat Commun 2020;11(1):3232.
[121] Rosenblum D, Gutkin A, Kedmi R, Ramishetti S, Veiga N, Jacobi A, et al. CRISPR-Cas9 genome editing using targeted lipid nanoparticles for cancer therapy. Sci Adv 2020;6(47):eabc9450.
[122] Liu X, Erikson RL. Polo-like kinase (Plk)1 depletion induces apoptosis in cancer cells. Proc Natl Acad Sci USA 2003;100(10):5789–94.
[123] Winkles JA, Alberts GF. Differential regulation of polo-like kinase 1, 2, 3, and 4 gene expression in mammalian cells and tissues. Oncogene 2005;24(2):260–6.
[124] Yin H, Song C, Dorkin JR, Zhu LJ, Li Y, Wu Q, et al. Therapeutic genome editing by combined viral and non-viral delivery of CRISPR system components in vivo. Nat Biotechnol 2016;34(3):328–33.
[125] Farbiak L, Cheng Q, Wei T, Álvarez-Benedicto E, Johnson LT, Lee S, et al. All-in-one dendrimer-based lipid nanoparticles enable precise HDR-mediated gene editing in vivo. Adv Mater 2021;33(30):e2006619.
[126] Nguyen DN, Roth TL, Li PJ, Chen PA, Apathy R, Mamedov MR, et al. Polymer-stabilized Cas9 nanoparticles and modified repair templates increase genome editing efficiency. Nat Biotechnol 2020;38(1):44–9.
[127] Musunuru K, Chadwick AC, Mizoguchi T, Garcia SP, DeNizio JE, Reiss CW, et al. In vivo CRISPR base editing of PCSK9 durably lowers cholesterol in primates. Nature 2021;593(7859):429–34.
[128] Gaudelli NM, Lam DK, Rees HA, Solá-Esteves NM, Barrera LA, Born DA, et al. Directed evolution of adenine base editors with increased activity and therapeutic application. Nat Biotechnol 2020;38(7):892–900.
[129] Rothgangl T, Dennis MK, Lin PJC, Oka R, Witzigmann D, Villiger L, et al. In vivo adenine base editing of PCSK9 in macaques reduces LDL cholesterol levels. Nat Biotechnol 2021;39(8):949–57.
[130] Villiger L, Rothgangl T, Witzigmann D, Oka R, Lin PJC, Qi W, et al. In vivo cytidine base editing of hepatocytes without detectable off-target mutations in RNA and DNA. Nat Biomed Eng 2021 Feb 1;5(2):179–89.
[131] Villiger L, Grisch-Chan HM, Lindsay H, Ringnalda F, Pogliano CB, Allegri G, et al. Treatment of a metabolic liver disease by in vivo genome base editing in adult mice. Nat Med 2018;24(10):1519–25.
[132] Gootenberg JS, Abudayyeh OO, Lee JW, Essletzbichler P, Dy AJ, Joung J, et al. Nucleic acid detection with CRISPR-Cas13a/C2c2. Science 2017;356(6336):438–42.
[133] Abudayyeh OO, Gootenberg JS, Konermann S, Joung J, Slaymaker IM, Cox DBT, et al. C2c2 is a single-component programmable RNA-guided RNA-targeting CRISPR effector. Science 2016;353(6299):aaf5573.
[134] Abudayyeh OO, Gootenberg JS, Essletzbichler P, Han S, Joung J, Belanto JJ, et al. RNA targeting with CRISPR-Cas13. Nature 2017;550(7675):280–4.
[135] Blanchard EL, Vanover D, Bawage SS, Tiwari PM, Rotolo L, Beyersdorf J, et al. Treatment of influenza and SARS-CoV-2 infections via mRNA-encoded Cas13a in rodents. Nat Biotechnol 2021;39(6):717–26.
[136] Pardi N, Secreto AJ, Shan X, Debonera F, Glover J, Yi Y, et al. Administration of nucleoside-modified mRNA encoding broadly neutralizing antibody protects humanized mice from HIV-1 challenge. Nat Commun 2017;8:14630.
[137] Kose N, Fox JM, Sapparapu G, Bombardi R, Tennekoon RN, Dharshan De Silva A, et al. A lipid-encapsulated mRNA encoding a potently neutralizing human monoclonal antibody protects against chikungunya infection. Sci Immunol 2019;4(35):eaaw6647.
[138] Rybakova Y, Kowalski PS, Huang Y, Gonzalez JT, Heartlein MW, DeRosa F, et al. mRNA delivery for therapeutic anti-HER2 antibody expression in vivo. Mol Ther 2019;27(8):1415–23.
[139] Wang Y, Tiruthani K, Li S, Hu M, Zhong G, Tang Y, et al. mRNA delivery of a bispecific single-domain antibody to polarize tumor-associated macrophages and synergize immunotherapy against liver malignancies. Adv Mater 2021;33(23):e2007603.
[140] Hewitt SL, Bai A, Bailey D, Ichikawa K, Zielinski J, Karp R, et al. Durable anticancer immunity from intratumoral administration of IL-23, IL-36γ, and OX40L mRNAs. Sci Transl Med 2019;11(477):eaat9143.
[141] Jiang L, Park J, Yin L, Laureano R, Jacquinet E, Yang J, et al. Dual mRNA therapy restores metabolic function in long-term studies in mice with propionic acidemia. Nat Commun 2020;11(1):5339.
[142] Riley RS, Kashyap MV, Billingsley MM, White B, Alameh M, Bose SK, et al. Ionizable lipid nanoparticles for in utero mRNA delivery. Sci Adv 2021;7(3):eaba1028.
[143] Lokugamage MP, Gan Z, Zurla C, Levin J, Islam FZ, Kalathoor S, et al. Mild innate immune activation overrides efficient nanoparticle-mediated RNA delivery. Adv Mater 2020;32(1):e1904905.
[144] Paunovska K, da Silva Sanchez A, Foster MT, Loughrey D, Blanchard EL, Islam FZ, et al. Increased PIP3 activity blocks nanoparticle mRNA delivery. Sci Adv 2020;6(30):eaba5672.